JOURNAL OF SOLID STATE CHEMISTRY 120, 231–237 (1995)

A New Silicate Clathrate Hydrate: An X-Ray Diffraction and Nuclear Magnetic Resonance Study of a System with Octameric Silicate Anions and Trivalent Cations

Robin K. Harris,[1] Judith A. K. Howard, Abdolraouf Samadi-Maybodi, and Jing Wen Yao

Department of Chemistry, University of Durham, South Road, Durham DH1 3LE, United Kingdom

and

Warren Smith

BP Chemicals Ltd., Research Laboratory, Chertsey Road, Sunbury-on-Thames, Middlesex TW16 7LN, United Kingdom

Received March 27, 1995; in revised form June 6, 1995; accepted June 9, 1995

The first crystal structure is reported for a silicate clathrate hydrate involving a triply charged cation $[C_{18}H_{30}N_3]^{3+}$ and an octameric cubic silicate cage. The structure is essentially a host/guest system, with the silicate cages linked into a framework by hydrogen bonding to water molecules. The space group is $P\bar{1}$ with $Z = 2$, and the asymmetric unit includes a complete cation and half the anion, plus 21 water molecules (4 of which are in disordered positions). Solid-state (CPMAS) ^{29}Si and ^{13}C NMR spectra are consistent with the diffraction-determined structure and indicate substantial distortion of the anion from cubic symmetry. Solution-state spectra of precursor solutions and of melted material are also presented and discussed. © 1995 Academic Press, Inc.

INTRODUCTION

The search for detailed understanding of the mechanisms of formation of zeolites has, over the past 2 decades, prompted many investigations into the species present in silicate solutions (with or without aluminate) and in solids obtained therefrom. The vital role played by nitrogen-containing cations as templates in hydrothermal zeolite synthesis has focused attention on systems including these components. It is well-known that such cations stabilize cagelike silicate anions, for instance the so-called prismatic hexamer $Si_6O_{15}^{6-}$ and cubic octamer $Si_8O_{20}^{8-}$ (and their various protonated forms). From such solutions a variety of crystalline hydrates can be obtained. Recently these have been shown to have network topologies involving host–guest considerations, i.e., they are clathrates. The host structures of these materials are three-dimensional tetrahedral networks. The frameworks involve either covalent bonding (Si–O–Si) or hydrogen bonding (Si–O–H···O–Si, H–O–H···O–Si or H–O–H···OH_2). Parallels are being suggested between these clathrate hydrates and zeolites. In particular, a series of papers by Wiebcke and coworkers has established the crystal structures of five systems involving the cubic octamer, namely,

$[NMe_4]_8[Si_8O_{20}]\cdot 65H_2O$ (see Refs. (1, 2)) [1]

$[NMe_4]_{16}[Si_8O_{20}][OH]_8\cdot 116H_2O$ (see Ref. (3)) [2]

$[DMPI]_6[SiO_{18}(OH)_2]\cdot 48.5H_2O$ (see Ref. (4)) [3]

$[TMPA]_4[Si_8O_{20}]\cdot 34H_2O$ (see Ref. (5)) [4]

$[DDBO]_4[Si_8O_{20}]\cdot 32H_2O$ (see Ref. (5)), [5]

where

DMPI is 1,1-dimethylpiperidinium [6]

TMPA is 1,1,4,4-tetramethylpiperazinium [7]

DDBO is 1,4-dimethyl-1,4-diazoniabicyclo[2.2.2]octane. [8]

Clearly [1], [2], and [3] contain singly charged cations, whereas [4] and [5] have doubly charged cations. However, in all cases a stable host–guest network is obtained. As part of an ongoing investigation into the synthesis of novel zeolites, we have aimed to produce a silicate clathrate hydrate containing the cubic octameric silicate anion with triply-charged cations. We have succeeded in crystallizing a novel product with molecular formula

[1] To whom correspondence should be addressed.

0022-4596/95 $12.00

$$[HMBPT]_2[Si_8O_{18}(OH)_2]\cdot 41H_2O, \quad [9]$$

where

HMBPT is 2,3,4,5,6,7,8,9-octahydro-
2,2,5,5,8,8-hexamethyl-1H-benzo
(1,2-c:3,4-c′:5,6-c″)tripyrrolium. [10]

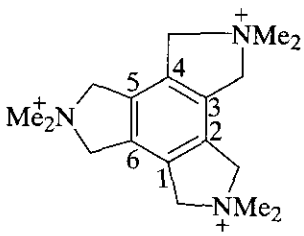

[10]

The cation [10] ($C_{18}H_{30}N_3$) has been referred to as triquat (6). The synthesis of its tribromide and the crystal structure of the tribromide dihydrate have been described (6, 7). The cation has been used in the synthesis of zeolites ZSM-18 (8) and SUZ-9 (9). The structure of the former contains trimeric [(Si, Al)–O]$_3$ rings (10). Here we report the full crystal structure and magic-angle spinning (MAS) NMR spectra of [9].

EXPERIMENTAL

Synthesis. A triquat bromide solution was prepared by the method of Ciric *et al.* (7) via the synthesis of hexakis(bromoethyl)benzene. The bromide was converted to hydroxide by dissolving in the minimum amount of water and passing down a column of Aldrich amberlite resin IRA-400 (OH), carefully neutralized beforehand. Elution with distilled water was carried out until the liquid was at pH 7. The water was then removed under reduced pressure. A clear solution with a molar ratio HMBPT:SiO_2 of 1:4 was prepared at ca. 60°C (with standing for 2 days) from HMBPT hydroxide, silica, and deionized water. This solution was examined by NMR at several temperatures. The water contained 15% (w/w) D_2O to give a ^2D field/frequency lock signal. Crystals of $[HMBPT]_2[Si_8O_{18}(OH)_2]\cdot 41H_2O$ were obtained by cooling the solution to ca. 15°C. Since the crystals dehydrated/decomposed in air, they were stored under the mother liquor in a polyethylene container. C, H, and N analysis (Elemental Analyzer model 1106) gave results within 6% of the empirical formula for the hydrate.

Diffraction measurements. An appropriate single crystal, approximately 0.7 × 0.5 × 0.4 mm in size, was selected and mounted on a RIGAKU AFC6S diffractometer operating at 150 K with graphite-crystal monochromatized Mo$K\alpha$ X-radiation (λ = 0.71073 Å). The structure was initially solved by direct methods (SHELXL-86) and successfully completed by full-matrix least-squares refinement with F_0^2 (SHELXL-93) and Fourier difference syntheses. A total of 6362 independent reflections were used. These were weighted as $w = 1/[\sigma^2(F_o^2) + (aP)^2 + bP]$ where $P = [\max(F_o^2, 0) + 2F_c^2]/3$, a = 0.051, and b = 3.814 in the final cycles. The final R factor for F^2 was wR_2 = 0.108 and for F was R = 0.042 for $[I > 2\sigma(I)]$, with wR_2 = 0.124 for F^2 and R = 0.074 for F for all 6362 data, including some hydrogen atoms (e.g., those on HMBPT) in the refinement.

TABLE 1
Crystal Data and Structure Refinement for Compound [9]

Identification code	S100
Chemical formula	$(C_{18}H_{30}N_3)_2\cdot[Si_8O_{18}(OH)_2]\cdot 41H_2O$
Formula weight	1862.34
Temperature	150(2) K
Wavelength	0.71073 Å
Crystal system	Triclinic
Space group	$P\bar{1}$
Unit cell dimensions	a = 12.910(6) Å, α = 100.76(4)° b = 13.699(6) Å, β = 114.77(4)° c = 13.945(6) Å, γ = 94.55(5)°
Volume	2165(2) Å^3
Z	2
Number of reflections used	20
Crystal description	Block
Crystal color	Colorless
Density (calculated)	1.440 mg/m^3
Absorption coefficient	0.236 mm^{-1}
$F(000)$	1010
Crystal size	0.7 × 0.5 × 0.4 mm
θ range for data collection	2.52 to 24.97°
Index ranges	$-15 \leq h \leq 15$, $0 \leq k \leq 14$, $-16 \leq l \leq 16$
Experiment device	Rigaku AFC6S
Experiment method	ω
Number of standard reflections	3
Interval counts	150
Reflections collected	6712
Independent reflections	6362 [R_{int} = 0.0198]
Absorption correction	Empirical
Refinement method	Full-matrix least-squares on F^2
Data/restraints/parameters	6362/0/543
Goodness-of-fit on F^2	1.036
Final R indices $[I > 2\sigma(I)]$	R_1 = 0.0423, wR_2 = 0.1078
R indices (all data)	R_1 = 0.0743, wR_2 = 0.1241
Largest diff. peak and hole	1.019 and −0.429 e Å^{-3}

NMR measurements. High-resolution ^{29}Si and ^{13}C spectra were obtained for the powdered polycrystalline solid at 59.58 and 75.43 MHz, respectively, using cross-polarization and magic-angle spinning (CPMAS) at ca. 273 K. The crystals were first dried between filter papers and packed into a 7.0-mm-o.d. zirconia rotor. A Varian Unity Plus 300 spectrometer was used. The spectrometer operating conditions were: contact time 10 msec (^{29}Si) and 3 msec (^{13}C); recycle delay 5 sec (^{29}Si) and 2 sec (^{13}C); num-

TABLE 2
Fractional Coordinates (× 10^4) and Equivalent Isotropic Displacement Parameters U_{eq} (Å^2 × 10^3) for Compound [9]

	x	y	z	U_{eq}[a]
Si(1)	6988(1)	1420(1)	6147(1)	14(1)
Si(2)	6288(1)	−104(1)	3935(1)	14(1)
Si(3)	3755(1)	353(1)	3002(1)	13(1)
Si(4)	4427(1)	1882(1)	5238(1)	13(1)
O(1)	6883(2)	649(2)	6871(2)	23(1)
O(2)	6992(2)	752(2)	5048(2)	25(1)
O(3)	5066(2)	177(2)	3197(2)	22(1)
O(4)	3883(2)	1306(2)	3953(2)	21(1)
O(5)	5821(2)	1916(2)	5761(2)	24(1)
O(6)	3893(2)	1186(2)	5814(2)	26(1)
O(11)	8107(2)	2256(2)	6805(2)	20(1)
O(12)	7070(2)	−180(2)	3275(2)	21(1)
O(13)	3068(2)	540(2)	1833(2)	19(1)
O(14)	4131(2)	2981(2)	5405(2)	18(1)
N(1)	6427(2)	2492(2)	−583(2)	18(1)
N(2)	6730(2)	3529(2)	3777(2)	18(1)
N(3)	10093(2)	1153(2)	3002(2)	21(1)
C(1)	7853(3)	2296(3)	1076(3)	19(1)
C(2)	7221(3)	3003(3)	1326(3)	17(1)
C(3)	7293(3)	3262(3)	2363(3)	17(1)
C(4)	8011(3)	2817(3)	3170(3)	16(1)
C(5)	8656(3)	2136(3)	2931(3)	17(1)
C(6)	8578(3)	1869(3)	1879(3)	19(1)
C(11)	5453(3)	1659(3)	−837(3)	24(1)
C(12)	6223(3)	2822(3)	−1607(3)	27(1)
C(13)	6655(3)	4309(3)	4649(3)	29(1)
C(14)	5762(3)	2649(3)	3375(3)	25(1)
C(15)	11153(3)	1924(3)	3323(3)	29(1)
C(16)	10467(3)	171(3)	3225(3)	32(1)
C(21)	7583(3)	2116(3)	−107(3)	22(1)
C(22)	6499(3)	3347(3)	324(3)	20(1)
C(23)	6679(3)	3950(3)	2825(3)	21(1)
C(24)	7888(3)	3163(3)	4193(3)	20(1)
C(25)	9431(3)	1537(3)	3637(3)	23(1)
C(26)	9270(3)	1053(3)	1809(3)	25(1)
O(51)	3694(2)	9639(2)	8600(2)	30(1)
O(52)	4103(3)	798(2)	622(2)	35(1)
O(53)	3403(3)	3813(2)	3690(2)	42(1)
O(54)	2611(2)	2406(2)	1734(2)	29(1)
O(55)	4235(2)	5443(2)	3160(2)	30(1)
O(56)	433(3)	2872(3)	964(3)	51(1)
O(57)	799(2)	9667(2)	796(3)	45(1)
O(58)	234(2)	7922(2)	1288(2)	40(1)
O(59)	2009(2)	5840(2)	2492(2)	36(1)
O(510)	8458(3)	8372(2)	3638(3)	47(1)
O(61)	6322(3)	6121(3)	1573(3)	56(1)
O(62A)[b]	8183(4)	−1766(7)	1484(4)	47(2)
O(62B)[b]	8292(11)	−2401(17)	1368(10)	31(4)
O(63A)[b]	1135(5)	5478(8)	248(4)	73(3)
O(63B)[b]	1141(11)	4748(17)	325(10)	44(5)
O(64A)[b]	8409(7)	5525(4)	1522(8)	67(3)
O(64B)[b]	8152(17)	5875(20)	889(19)	93(9)
O(67A)[b]	9444(14)	5370(14)	3290(13)	56(4)
O(67B)[b]	8897(18)	5491(16)	2732(18)	59(6)
O(65)	470(4)	4395(3)	2661(3)	81(1)
O(66)	754(4)	4242(3)	4786(4)	88(1)
O(68)	148(3)	7230(3)	3656(4)	77(1)
O(69)	4330(3)	4852(2)	1152(2)	46(1)
O(610)	3689(2)	2769(2)	474(2)	35(1)
O(611)	7401(2)	6658(2)	3844(2)	35(1)

[a] $U_{eq} = \frac{1}{3} \Sigma_i \Sigma_j U_{ij} \mathbf{a}_i \mathbf{a}_j \cdot a_i^* a_j^*$

[b] O(62A) occup. 75%, O(62B) occup. 25%; O(63A) occup. 75%, O(63B) occup. 25%; O(64A) occup. 75%, O(64B) occup. 25%; O(67A) occup. 27%, O(67B) occup. 23%.

ber of transients 200 (^{29}Si) and 750 (^{13}C); spin rate 2.4 kHz (^{29}Si) and 2.2 kHz (^{13}C).

Spectra for the precursor solution and of the mother liquor after crystallization were recorded at ca. 323 K and at ambient probe temperature (ca. 298 K), respectively, using a Bruker AC250 spectrometer operating at 49.69 and 62.90 MHz for ^{29}Si and ^{13}C, respectively. The general spectrometer operating conditions were: pulse angles 90° (^{29}Si) and 45° (^{13}C); recycle delay 50 sec (^{29}Si) and 35 sec (^{13}C); number of transients typically 1000–2000.

RESULTS AND DISCUSSION

Diffraction Measurements

The crystal structure of $[HMBTP]_2[Si_8O_{18}(OH)_2] \cdot 41H_2O$ was determined by X-ray diffraction methods. The crystal data and the relevant experimental parameters are listed in Table 1. The compound crystallizes in the triclinic space group $P\bar{1}$ (as does [1]), while [2] and [3] are trigonal, and [4] and [5] are monoclinic. Clearly there is little common morphology among these structures, which all appear to contain different numbers of water molecules per octameric silicate anion. The unit cell of [9] contains two triquat cations and one anionic cubic octamer. The refined coordinates of the Si, O, and N atoms are listed in Table 2. The asymmetric unit of [9] contains one triquat cation and half a cubic silicate octamer, together with 21 water oxygens. For the cations and anions this is similar to the situation for [4] and [5]. However, for [9] the best refinement model indicates that four of the water molecules are positionally disordered. Thus O(62), O(63), and O(64) show 3:1 site occupancy, while O(67) is almost equivalently split between two sites, which sum to 50% occupancy per asymmetric unit.

Table 3 gives the bond distances for the cations and anions, while Table 4 lists the relevant bond angles. Table 5 gives some additional geometry data in condensed form. The crystalline compound is clearly a host/guest system, as for the related molecules [1]–[5]. The anionic host struc-

TABLE 3
Bond Lengths (in Å) for the Anions and Cations of Compound [9]

Si(1)–O(11)	1.573(3)
Si(1)–O(5)	1.625(3)
Si(1)–O(1)	1.626(3)
Si(1)–O(2)	1.634(3)
Si(2)–O(2)	1.606(3)
Si(2)–O(3)	1.606(3)
Si(2)–O(6)[a]	1.607(3)
Si(2)–O(12)	1.623(2)
Si(3)–O(13)	1.578(3)
Si(3)–O(4)	1.621(3)
Si(3)–O(1)[a]	1.621(3)
Si(3)–O(3)	1.643(3)
Si(4)–O(14)	1.581(3)
Si(4)–O(5)	1.627(3)
Si(4)–O(4)	1.630(3)
Si(4)–O(6)	1.637(3)
O(1)–Si(3)[a]	1.621(3)
O(6)–Si(2)[a]	1.607(3)
N(1)–C(11)	1.503(5)
N(1)–C(12)	1.503(5)
N(1)–C(22)	1.520(4)
N(1)–C(21)	1.534(4)
N(2)–C(14)	1.501(5)
N(2)–C(13)	1.503(5)
N(2)–C(23)	1.522(4)
N(2)–C(24)	1.525(4)
N(3)–C(16)	1.507(5)
N(3)–C(15)	1.508(5)
N(3)–C(25)	1.523(4)
N(3)–C(26)	1.525(5)
C(1)–C(6)	1.387(5)
C(1)–C(2)	1.401(5)
C(1)–C(21)	1.502(5)
C(2)–C(3)	1.384(5)
C(2)–C(22)	1.506(5)
C(3)–C(4)	1.404(5)
C(3)–C(23)	1.501(5)
C(4)–C(5)	1.384(5)
C(4)–C(24)	1.494(5)
C(5)–C(6)	1.403(5)
C(5)–C(25)	1.500(5)
C(6)–C(26)	1.498(5)

[a] Symmetry transformations used to generate equivalent atoms: $-x + 1, -y, -z + 1$.

ture is a three-dimensional network of hydrogen-bonded octameric silicate units and water molecules. Figure 1 shows the local environment of the octameric silicate ion, which is centrosymmetric and contains 22 water molecules, in contrast to [4] and [5] which have 24—possibly because [9] contains $[Si_8O_{18}(OH)_2]^{6-}$ anions (whereas [4] and [5] have $[Si_8O_{20}]^{8-}$ anions) or possibly because of the size of the cation [10]. This situation breaks the "24 water molecules" rule suggested in Ref. (5). Each external Si–O

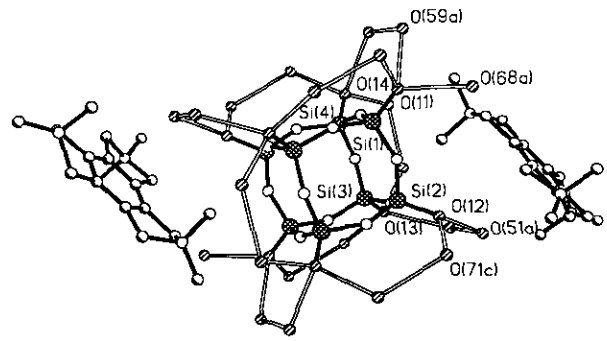

FIG. 1. The environment of the octameric silicate unit $[Si_8O_{18}(OH)_2]^{6-}$ in the crystal structure of compound [9]. The 22 water oxygen atoms linking to the silicate terminal oxygens are indicated.

oxygen is linked to others, intramolecularly, via two water molecules. However, whereas four of the terminal oxygens participate in three of these bridges, the other four (which are near to the cations) are only involved in two such links. Furthermore, of the latter four, two are bonded to only two water molecules, whereas the other two link to three. This is reflected in the Si–O distances, which are notably shorter (1.573–1.581 Å) for those terminal oxygens hydrogen-bonded to three water molecules than for those linked to two (1.623 Å). The internal Si–O distances are mostly in the region 1.621–1.643 Å, with those involving the silicon

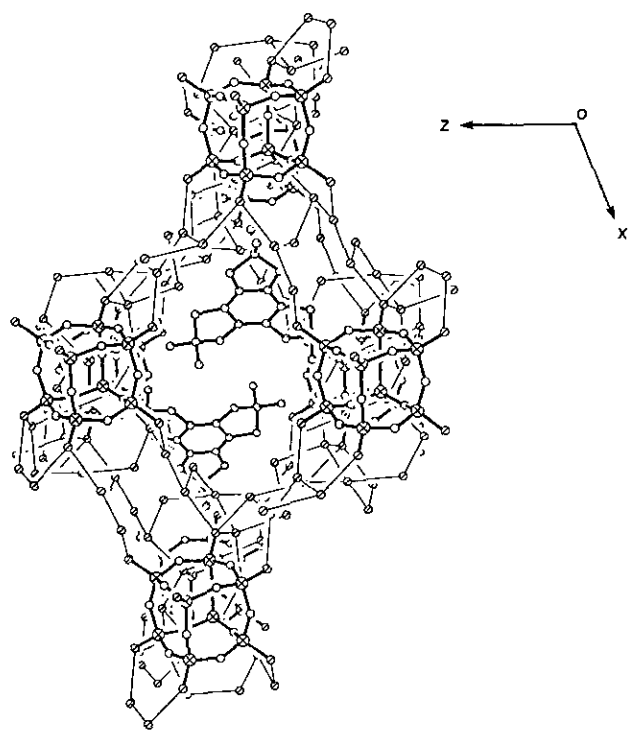

FIG. 2. The host–guest framework structure of compound [9].

TABLE 4
Bond Angles (in Degrees) for the Anions and Cations of Compound [9]

O(11)–Si(1)–O(5)	111.31(14)
O(11)–Si(1)–O(1)	111.54(14)
O(5)–Si(1)–O(1)	107.70(14)
O(11)–Si(1)–O(2)	111.27(14)
O(5)–Si(1)–O(2)	107.04(14)
O(1)–Si(1)–O(2)	107.77(14)
O(2)–Si(2)–O(3)	111.1(2)
O(2)–Si(2)–O(6)[a]	110.6(2)
O(3)–Si(2)–O(6)[a]	110.9(2)
O(2)–Si(2)–O(12)	107.69(14)
O(3)–Si(2)–O(12)	109.19(13)
O(6)[a]–Si(2)–O(12)	107.19(14)
O(13)–Si(3)–O(4)	111.67(14)
O(13)–Si(3)–O(1)[a]	110.92(14)
O(4)–Si(3)–O(1)[a]	108.88(14)
O(13)–Si(3)–O(3)	110.01(13)
O(4)–Si(3)–O(3)	107.74(14)
O(1)[a]–Si(3)–O(3)	107.47(14)
O(14)–Si(4)–O(5)	111.10(14)
O(14)–Si(4)–O(4)	111.80(13)
O(5)–Si(4)–O(4)	107.64(14)
O(14)–Si(4)–O(6)	110.78(13)
O(5)–Si(4)–O(6)	108.29(14)
O(4)–Si(4)–O(6)	107.1(2)
Si(3)[a]–O(1)–Si(1)	151.2(2)
Si(2)–O(2)–Si(1)	147.0(2)
Si(2)–O(3)–Si(3)	149.8(2)
Si(3)–O(4)–Si(4)	150.2(2)
Si(1)–O(5)–Si(4)	154.4(2)
Si(2)[a]–O(6)–Si(4)	147.6(2)
C(11)–N(1)–C(12)	108.7(3)
C(11)–N(1)–C(22)	109.1(3)
C(12)–N(1)–C(22)	112.7(3)
C(11)–N(1)–C(21)	109.3(3)
C(12)–N(1)–C(21)	112.1(3)
C(22)–N(1)–C(21)	104.9(3)
C(14)–N(2)–C(13)	109.4(3)
C(14)–N(2)–C(23)	109.6(3)
C(13)–N(2)–C(23)	112.3(3)
C(14)–N(2)–C(24)	109.5(3)
C(13)–N(2)–C(24)	111.7(3)
C(23)–N(2)–C(24)	104.2(3)
C(16)–N(3)–C(15)	108.8(3)
C(16)–N(3)–C(25)	111.3(3)
C(15)–N(3)–C(25)	109.6(3)
C(16)–N(3)–C(26)	112.8(3)
C(15)–N(3)–C(26)	108.9(3)
C(25)–N(3)–C(26)	105.4(3)
C(6)–C(1)–C(2)	119.9(3)
C(6)–C(1)–C(21)	130.2(3)
C(2)–C(1)–C(21)	109.9(3)
C(3)–C(2)–C(1)	120.5(3)
C(3)–C(2)–C(22)	129.7(3)
C(1)–C(2)–C(22)	109.8(3)
C(2)–C(3)–C(4)	119.6(3)
C(2)–C(3)–C(23)	131.1(3)
C(4)–C(3)–C(23)	109.2(3)
C(5)–C(4)–C(3)	119.9(3)
C(5)–C(4)–C(24)	130.2(3)
C(3)–C(4)–C(24)	109.8(3)
C(4)–C(5)–C(6)	120.4(3)
C(4)–C(5)–C(25)	129.3(3)
C(6)–C(5)–C(25)	110.1(3)
C(1)–C(6)–C(5)	119.6(3)
C(1)–C(6)–C(26)	130.4(3)
C(5)–C(6)–C(26)	109.7(3)
C(1)–C(21)–N(1)	101.9(3)
C(2)–C(22)–N(1)	102.0(3)
C(3)–C(23)–N(2)	102.0(3)
C(4)–C(24)–N(2)	102.2(3)
C(5)–C(25)–N(3)	102.5(3)
C(6)–C(26)–N(3)	102.4(3)

[a] Symmetry transformations used to generate equivalent atoms: $-x + 1$, $-y$, $-z + 1$.

atoms whose terminal oxygen atoms participate in only two hydrogen bonds distinctly shorter (1.606–1.607 Å). It is tempting to suppose that these silicon atoms are those with OH groups, but we have no direct evidence of this, and presumably the H-bonding network can in principle delocalize the charges. For [5] and [6] all Si–O bonds to terminal oxygen atoms are in the range 1.570–1.588 Å,

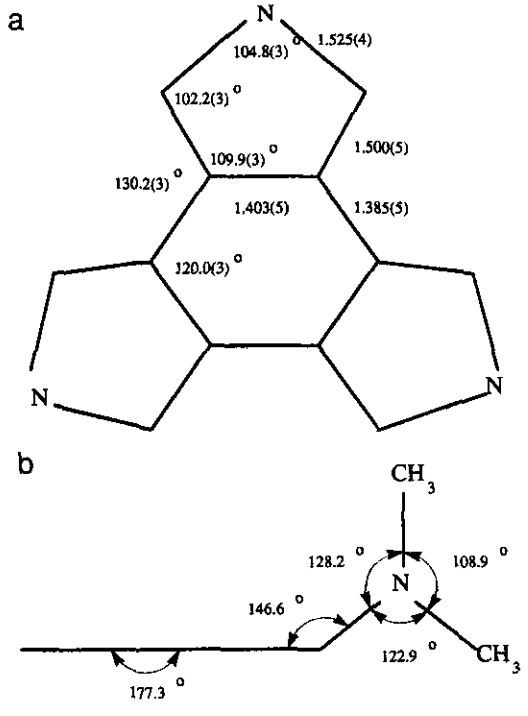

FIG. 3. The average bond distances and angles (in Å and degrees respectively) in the triquat cation, [10], of compound [9]: (a) the cyclic skeleton, and (b) the nitrogen environment.

TABLE 5
Geometry Data for Compound [9]

	Average value	Range of values
$Si-O_{br}$	1.622(3) Å	1.606(3)–1.643(3) Å
$Si-O_{term}$	1.589(3) Å	1.573(3)–1.623(3) Å
$O_{br}-Si-O_{br}$	108.5(1)°	107.04(14)–111.1(2)°
$O_{br}-Si-O_{term}$	110.37(14)°	107.19(14)–111.80(13)°
$Si-O_{br}-Si$	150.0(2)°	147.0(2)–154.4(2)°
$O_w \cdots O_{term}$	2.676(5) Å	2.609(4)–2.756(5) Å
$O_w \cdots O_w$	2.72(2) Å	2.26(2)–2.92(3)Å

whereas the other cage Si–O bond lengths lie in the range 1.612–1.628 Å.

Figure 2 shows the complex hydrogen-bonded network linking silicate anions. Each structure of this type so far examined in detail contains a different number of water molecules, presumably to accommodate the different cation shapes within a stable framework. Table 5 gives some data for the hydrogen-bonded O–O distances for [9], which show an anticipated range of values. The framework shown in Fig. 2 reveals large irregular cagelike cavities, which contain the guest triquat cations. The high charge but large size of these cations means there are fewer but more substantial breaks in the host framework than is the case for structures [1]–[5]. The cations are almost planar (apart from the methyl groups). Figure 3 gives average bond lengths and bond angles for the cation in [9]. These are close to those for the bromide (6, 7), but for [9] it would appear that there is a small alternation in the bond lengths of the central C_6 ring.

NMR Spectra

Silicon-29 NMR spectra of the precursor solution at ca. 323 K and of the mother liquor (i.e., saturated solution after crystallization) at ca. 298 K are shown in Fig. 4. They were recorded using a substantial recycle delay (50 sec) to obtain quantitative data. Measurements of a number of HMBPT:silica solutions showed a range of relaxation times, the maximum value of T_1 being ca. 9 sec. It can be seen that a wide range of silicon environments is present in both cases. This contrasts with the situation reported in Ref. (5). As usual for alkaline silicate signals, separate bands are visible in Fig. 5 for Q^0, Q^1, Q^2_Δ, Q^2/Q^3_Δ, and Q^3 sites, where the superscript gives the number of siloxane bridges and the subscript triangle refers to three-membered $(SiO)_3$ rings. Peaks assignable (11) to the individual species Q^0, Q^1_2, Q^2_3, Q^3_6, and Q^3_8, (known as the monomer, dimer, cyclic trimer, prismatic hexamer, and cubic octamer, respectively) are of substantial intensity. In general the spectrum of the mother liquor contains less intensity arising from condensed units, as expected because of the lower

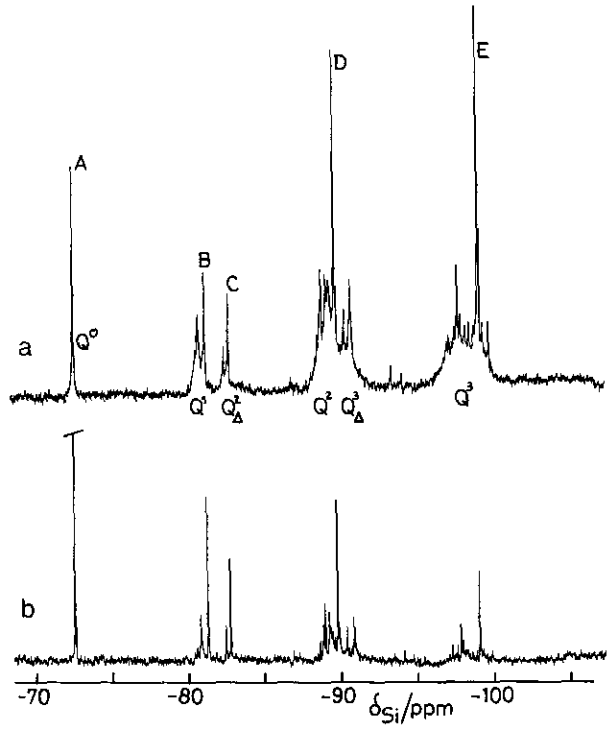

FIG. 4. The 49.69 MHz ^{29}Si NMR spectra of triquat silicate solutions: (a) at ca. 323 K prior to crystallization, (b) the mother liquor at ca. 298 K after crystallization. Spectrometer operating conditions: Number of transients 1300 (a) and 1424 (b); recycle delay 50 sec. In (b) the Q^0 peak has been terminated below its maximum height. The Q notation for the different bands is described in the text. Individual resonances A to E are assigned, in order, to Q^0, Q^1_2, Q^2_3, Q^3_6, and Q^3_8.

total concentration of silicate. The spectrum of the precursor solution is not as well resolved as that of the mother liquor because chemical exchange occurs more readily at the temperature used for the former. The crystalline material was later melted and the ^{29}Si spectrum obtained at ca. 355 K (Fig. 5). This liquid has a high silicate:water molar

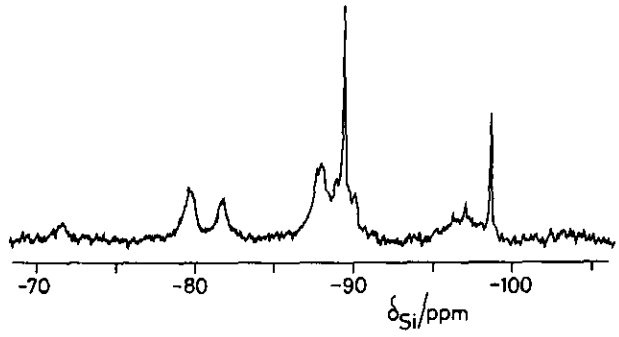

FIG. 5. The 49.69 MHz ^{29}Si NMR spectrum of the melted $[HMBPT]_2[Si_8O_{18}(OH)_2]\cdot 41H_2O$ at ca. 355 K. A recycle delay of 50 sec was used with 1320 transients.

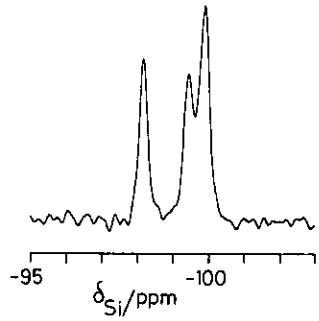

FIG. 6. The 59.58 MHz CPMAS ^{29}Si NMR spectrum of solid [9] at ambient probe temperature. For the operating conditions, see the Experimental section.

ratio of 8:42 (the latter figure including the hydroxyl groups) and a silica:cation charge ratio of 4:3 (identical to that of the precursor solution). The spectrum shows many species are present, with broad lines (indicating relatively facile exchange) except for the Q_6^3 and Q_8^3 peaks (which demonstrates their stability). Evidently a distribution of species is rapidly regained on melting.

Figure 6 displays the 59.58 MHz CPMAS ^{29}Si spectrum of the powdered solid [9] at 273 K. Three peaks can be seen at chemical shifts $\delta_{Si} = -99.9, -99.5$, and -98.2 ppm from the signal for Me_4Si, the one at -99.9 ppm being broader than and twice as intense as the others. The shifts for the cubic octamer in the spectra of the precursor solution and the mother liquor are -98.5 and -98.9 ppm, respectively, so there is little overall change on crystallization—not surprising as the dominant environment consists of water molecules in both solid and solution states. Evidently distortions in the cubic octamer cage in the solid state cause chemical shifts sufficient to distinguish the sites in the asymmetric unit. A recycle delay of only 5 sec and a contact time of 10 msec may not allow a fully quantitative spectrum to be obtained. However, the appearance of the peaks confirms that the crystal used for the diffraction study is likely to be typical of the whole microcrystalline sample obtained—a not unimportant result.

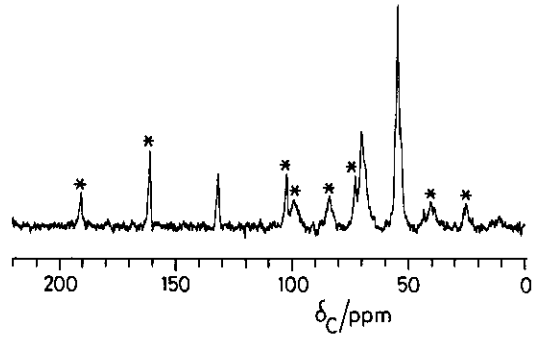

FIG. 7. The 75.43 MHz CPMAS ^{13}C NMR spectrum of solid [9] at ambient probe temperature. Asterisks indicate spinning sidebands. For the operating conditions, see the text.

Figure 7 shows the 75.43 MHz CPMAS ^{13}C spectrum of powdered [9]. Three major bands are seen, as expected, at δ_C ca. 54, 70, and 132 ppm assignable to the CH_3, CH_2, and quaternary carbon nuclei, respectively. However, all the peaks show evidence of shoulders. Once again, this is consistent with the crystal structure, which would indicate all 18 carbons are in nonequivalent sites—it is not to be expected that resolution would suffice to enable these to be clearly distinguished. Carbon-13 spectra of silicate solutions corresponding to [9] (e.g., after melting the solid) show sharp peaks at $\delta_C = 54.1, 69.8$, and 131.4 ppm. Evidently there are no substantial changes in shift on crystallization, presumably because both in solution and in the solid state the immediate environment of the triquat ion is composed of water molecules.

ACKNOWLEDGMENTS

One of us (A.S-M.) thanks the Iranian Ministry of Culture and Higher Education for a Studentship. Another (J.W.Y.) is grateful for financial assistance from the University of Durham. We acknowledge support from the U.K. Science & Engineering Research Council for the purchase of the Chemagnetics CPMAS spectrometer under Grant CG/H-96096.

REFERENCES

1. M. Wiebcke, *J. Chem. Soc. Chem. Commun.*, 1507 (1991).
2. M. Wiebcke, M. Grube, H. Koller, G. Engelhardt, and J. Felsche, *Microporous Mater.* **2,** 55 (1993).
3. M. Wiebcke and D. Hoebbel, *J. Chem. Soc. Dalton Trans.*, 2451 (1992).
4. M. Wiebcke, J. Emmer, and J. Felsche, *Chem. Soc. Chem. Commun.*, 1604 (1993).
5. M. Wiebcke, J. Emmer, J. Felsche, D. Hoebbel, and G. Engelhardt, *Z. Anorg. Allg. Chem.* **620,** 757 (1994).
6. S. L. Lawton, J. Ciric, G. T. Kokotailo, and G. W. Griffin, *Acta Crystallogr. Sect. C* **41,** 1683 (1985).
7. J. Ciric, S. L. Lawton, G. T. Kokotailo, and G. W. Griffin, *J. Am. Chem. Soc.* **100,** 2173 (1978).
8. J. Ciric, U.S. Patent 3 950 496 (1976).
9. U.S. Patent 5397561 (1995).
10. S. L. Lawton and W. J. Rohrbaugh, *Science* **247,** 1319 (1990).
11. R. K. Harris and C. T. G. Knight, *J. Chem. Soc. Faraday Trans. 2* **79,** 1525 (1983); **79,** 1539 (1983).